MAGNETIC RESONANCE IN CHEMISTRY
Magn. Reson. Chem. **36**, 815–825 (1998)

Membrane-induced conformation of [Val4, Ile7] angiotensin III by NMR and molecular dynamics methods

Anant B. Patel, Sudha Srivastava* and Ratna S. Phadke

Tata Institute of Fundamental Research, Homi Bhabha Road, Colaba Mumbai-400005, India

Received 28 October 1997; Revised 8 April 1998; Accepted 15 May 1998

ABSTRACT: The conformation of [Val4, Ile7]Angiotensin III has been studied in aqueous and micellar (DPC) media by 2D NMR and MD simulations. Complete resonance assignments have been made using combination of DQF-COSY, TOCSY and ROESY/NOESY spectra. The NMR parameters – $^3J_{NH}$ coupling constants, deuterium exchange rates, chemical shifts and the pattern of intra and inter-residue NOEs together with the restrained MD simulations show that the molecule acquires an extended conformation in water and a conformation in DPC micelles which is characterized by a bend at Val4. © 1998 John Wiley & Sons, Ltd.

KEYWORDS: NMR; ^{1}H NMR; angiotensin III analogue; iterative relaxation matrix approach; IRMA; molecular dynamics; conformation; dodecylphosphocholine micelles

INTRODUCTION

Endogenous peptide neurotransmitters in general and enkephalin in particular are reported to be rapidly inactivated by enzymes such as angiotensin-converting enzyme (ACE), membrane-bound diaminopeptidases and aminopeptidases after their release by neurons. On the other hand, it has been suggested that dipeptidylaminopeptidase and aminopeptidase are essential for the degradation of enkephalin. Angiotensin derivatives having a basic or neutral amino acid at the *N*-terminus show strong inhibition. The most potent inhibitor of dipeptidylaminopeptidase and aminopeptidase has been found to be angiotensin III. It also displays analgesic activity. This prompted us to examine various polypeptides such as the angiotensins, bradykinins and related peptides regarding their role as inhibitors of the enkephalin-degrading enzymes.[1]

Angiotensin III (Arg1–Val2–Tyr3–Ile4–His5–Pro6–Phe7) is one of the *in vivo* degradation products of angiotensin II (Asp1–Arg2–Val3–Tyr4–Ile5–His6–Pro7–Phe8), resulting from enzymatic cleavage of the Asp1–Arg2 bond by angiotensinase A_1 and A_2.[2] Angiotensin III is known to retain significant pressor and myotropic activity. It is also known to stimulate the synthesis of catecholamines and aldosterone *in vivo*.[2] Both angiotensin II and III have been the subject of a large number of studies in which various derivatives of the hormones have been prepared and their biological activities have been assayed[3] with a view to elucidating the role played by each amino acid residue in the peptide–receptor binding and triggering of physiological responses. The solution conformations of the native hormone and conformationally perturbed analogues are likely to provide clues for understanding the structure–function relationship useful in designing more potent analogues. With this in mind, we have determined the solution conformation of [Val4, Ile7]angiotensin III, i.e. (Arg1–Val2–Tyr3–Val4–His5–Pro6–Ile7) (VIA) analogue. It is pertinent to study the conformation of the peptide in membrane systems, as the enzymes (ACE) reside in the membrane, and the inhibitory action may be triggered by a specific conformation attained by the peptide when it is in membrane matrix rather than when in aqueous solution.

Nuclear magnetic resonance (NMR) spectroscopy offers a powerful method for the investigation of the structural details of macromolecules in solution.[4] The conformation or structure of the peptide in a membrane can be conveniently studied using a model system such as dodecylphosphocholine (DPC) micelles. Micelles are documented to possess inherent salient features of membranes, i.e. amphiphillicity and electrostatic potential.

EXPERIMENTAL

VIA was purchased from Sigma (USA) and was used in its original form as it was found to be pure when examined using NMR. Dodecylphosphocholine-d_{38} (DPC) was purchased from Cambridge Isotope Laboratories (USA).

For NMR studies, a solution of 5 mg of VIA dissolved in 0.6 ml of H_2O–D_2O (90:10) was used. The pH of the sample was adjusted to 3.8 to facilitate the observation of NH protons. Unless mentioned otherwise, all experiments were carried out at 298 K.

* *Correspondence to*: S. Srivastava, Tata Institute of Fundamental Research, Homi Bhabha Road, Colaba Mumbai-400005, India.
E-mail: sudha@tifrvax.tifr.res.in

CCC 0749-1581/98/110815–11 $17.50

Preparation of peptide-incorporated DPC micelles

A solution of DPC was prepared by dissolving 15 mg of DPC in 0.5 ml of chloroform. A thin film of DPC was prepared on the inner wall of a test-tube by first evaporating the solvent with a stream of dry nitrogen and then thoroughly drying under high vacuum. The film thus prepared was hydrated and equilibrated with a solution of the peptide (the DPC:peptide ratio used was maintained at 9:1). Micelles were prepared by mild sonication of this dispersion in a nitrogen atmosphere using a bath sonifier until the dispersion was optically clear. The optical clarity indicated that the dispersion contained small-sized micelles.

NMR experiments

NMR experiments were carried out on a Varian Unity Plus 600 MHz FT-NMR spectrometer operating at a ^{1}H resonance frequency of 600 MHz. Data were processed on Silicon Graphics Indigo workstation using Felix software (version 2.30) (MSI, USA).

For the unambiguous assignment of spin systems of the peptide, double quantum filtered correlated spectroscopy (DQF COSY)[5] experiment was performed in aqueous and micellar media. Total correlation spectroscopy (TOCSY),[6,7] nuclear Overhauser effect spectroscopy (NOESY)[8] and/or rotating frame nuclear Overhauser effect spectroscopy (ROESY)[9,10] were performed both on the pure peptide in aqueous solution and in the presence of micelles (TRNOESY) using standard pulse sequences. For the TOCSY experiment an MLEV17 mixing scheme of 80 ms with 13 kHz spin-lock field strength was used. The ROESY spectrum was recorded with a mixing time of 250 ms. Mixing was achieved by the continuous wave method with a field strength of 3 kHz. In all these experiments water was suppressed during the relaxation period with pules having the appropriate parameters. Unless indicated otherwise, all 2D NMR experiments were performed by hypercomplex (STATES) methods[11] using the conventional pulse sequences and a 1 s relaxation delay. The acquisition parameters used for 2D experiments were as follows: spectral width 6500 Hz, 512 and 2048 data points in t_1 and t_2 dimensions, respectively, and 16, 8 and 32 scans per t_1 increment for DQF-COSY, TOCSY and NOESY/ROESY experiments, respectively. The data were apodized with a sine-bell window function and zero-filled to a matrix of size of 2K × 1K data points prior to Fourier transformation

Molecular dynamics simulations

Calculations were done on a Silicon Graphics IRIS Indigo workstation with molecular modeling software (Insight II v. 2.3 and Discover v. 2.9) from MSI. The heptapeptide was built using the Biopolymer module. The energy of the system was calculated with the CVFF forcefield[12] and bond stretching was described by a harmonic approximation. No cross-terms were included in the energy expression. The dielectric constant was fixed at 80.0. A cut-off of 12 Å was used for the non-bonded energy evaluation. Calculations were done for pH = 3.7, at which NMR experiments were carried out.

NOE intensities and refinement of inter-proton distances

NOE intensities were determined using the integration routine in the FELIX program from TRNOE and ROE data measured during the linear part of the signal build-up. The inter-proton distances were calculated from the cross peak-volumes using the following relationship:[13–16]

$$r_{ij} = r_{kl}\left(\frac{I_{kl}}{I_{ij}}\right)^{1/6} \quad (1)$$

where r_{ij} and r_{kl} are the distances and I_{ij} and I_{kl} are the NOE intensities of the spins ij and kl, respectively. The δH_1 and δH_2 of the proline residue are non-degenerate and the internuclear distances of these protons will be independent of the conformation of the peptide. Therefore, this distance (1.85 Å) was taken as reference distance. Inter-proton distances thus calculated were refined by the iterative relaxation matrix approach (IRMA).[17] The initial structural model from a set of approximate distance constraints (derived from NOE data) was built using Insight. Constrained energy minimization and MD simulation was carried out with the following protocol. The molecule was energy minimized using the steepest descent method (100 iterations) followed by conjugate gradient (500 iterations). The MD simulation was performed on the minimized structure and 50 structures were generated. These structures were further energy minimized using the steepest descent and conjugate gradient methods to achieve an energy derivative of less than 0.01 kcal mol^{-1} Å^{-1}. The lowest energy structure from these structures was selected for IRMA analysis.

IRMA calculation was performed for both the data systems, i.e. peptide in water and in micellar medium. Local mobility, aromatic ring flips and methyl group rotation were taken into account in the calculation. The overall correlation time used was 0.3 ns as estimated from the size of the molecule. Each MD calculation was started with 100 steps of steepest-descent restrained energy minimization followed by 500 steps of conjugate gradients. Other computational conditions were temperature 300 K and time step 0.005 ps. Each MD run covered a time span of 2 ps, of which the last 1 ps was used for averaging. The averaged energy structure was again energy minimized using 100 steps of steepest descent and 1500 steps of conjugate gradients. After each cycle a new IRMA calculation was performed and distance constraints were updated. The process was repeated until convergence was achieved. The two criteria used for convergence were the *R*-factor and r.m.s.

differences in the atom coordinates between the structures.

Energy minimization

A total of 50 and 34 refined distances for water and micellar media, respectively, (Tables 1 and 2) were used as distance constraints by incorporating an additional harmonic term $K(R_{ij} - R_{\text{target}})^2$ to the forcefield. The force constant (k) was set to 90.0 kcal mol^{-1} Å^{-2}. The maximum force that was allowed to be used was 1000 kcal mol^{-1} to satisfy the constraints. The energy of the system was minimized first with 500 steps of steepest descent, followed by 1000 steps of conjugate gradients so as to remove any strain in the starting configuration. A forcing potential of 100 kcal mol^{-1} rad^{-2} was applied to all ω angles to keep them in a *trans* configuration during the simulation.

Newton's equation of motion were integrated with the Verlet algorithm with an integration time step of 1 fs.[18] The system was equilibrated at 600 K for 50 ps and dynamics continued for 100 ps at this temperature. Structures from the MD trajectory were sampled every 1 ps to generate 100 structures. Temperature control during equilibration was achieved by direct velocity scaling while during the sampling period (100 ps) a weak coupling to a temperature bath with a coupling constant of 0.1 ps was used. The structures generated at 600 K were slowly cooled to 300 K in different steps. Each cooling involves a reduction in temperature by 50 K followed by dynamics of 3 ps. At the end of the MD calculation all the stored 100 structures were energy minimized beginning with steepest descent followed by conjugate gradients until the derivative of energy fell below 0.01 kcal mol^{-1} Å^{-1}.

Hydrogen exchange

The kinetics of hydrogen exchange[19] were studied by dissolving the peptide in D_2O and measuring the signal height of individual NH resonances in the ^{1}H NMR spectrum as a function of time. In each case, 24 scans were accumulated at uniform time intervals over a period of 40 s. The intensity of each NH signal was observed to decrease exponentially with time, i.e. $I(t) = I(0)\exp(-kt)$, where k is the rate constant, $I(t)$ is the intensity at time t and $I(0)$ is the initial intensity. The exchange rates were obtained from least-squares analysis of the semi-logarithmic plots of signal height as a function of time. The activation energy for the deuterium exchange for different NH protons was calculated by performing the exchange study at different temperatures ranging from 277 to 292 K at intervals of 3 K. The observed exchange rate constant was fitted to the

Table 1. Inter-proton distances[a] (lower and upper bounds) for VIA in water

Proton pair	Distance (Å)		Proton pair	Distance (Å)	
His5:HE2–Ile7:HA	3.3	3.4	Val4:HN–His5:HN	3.6	5.6
Tyr3:HN–Tyr3:HA	3.1	3.2	His5:HN–Tyr3:HD[b]	3.6	4.0
Tyr3:HN–Val2:HA	2.1	2.2	Val4:HN–Tyr3:HE[b]	3.8	6.2
Tyr3:HN–Tyr3:HB2	2.4	2.7	His5:HD2–Tyr3:HD[b]	4.4	5.1
Val2:HN–Val2:HA	2.9	3.2	His5:HD2–Tyr3:HE[b]	4.4	4.8
Val2:HN–Arg:HA	2.3	2.4	Tyr3:HD*–Tyr3:HE[b]	1.9	2.7
Val2:HN–Val2:HB	2.7	2.8	His5:HA–Pro6:HD2	2.1	2.4
His5:HN–His5:HA	3.0	3.3	His5:HA–His5:HB2	2.7	3.1
His5:HN–Val4:HA	2.2	2.2	His5:HA–His5:HB1	2.9	2.9
His5:HN–His5:HB2	2.7	2.8	Tyr3:HA–Tyr3:HB2	3.0	3.5
Val4:HN–Tyr3:HA	2.3	2.3	Tyr3:HA–Tyr3:HB1	2.7	2.8
Val4:HN–Val4:HA	2.9	3.0	Pro6:HA–Pro6:HD2	3.7	4.7
Val4:HN–Val4:HB	2.6	2.6	Pro6:HA–Pro6:HB2	2.4	2.5
Ile7:HN–Pro6:HA	2.4	2.5	Pro6:HA–Pro6:HB1	2.6	2.9
Ile7:HN–Ile7:HA	3.2	3.5	Val2:HA–Val2:HB	2.5	2.6
Ile7:HN–Pro6:HB1	3.3	4.2	Ile7:HA–Ile7:HB	2.6	2.7
Ile7:HN–Ile7:HB	3.1	3.1	Ile7:HA–Ile7:HG2[b]	4.2	5.0
His5:HD2–His5:HA	3.5	4.0	Val4:HA–Val4:HB	2.5	2.5
His5:HD2–Pro6:HA	4.0	4.1	Pro6:HB1–Pro6:HD2	2.0	2.3
His5:HD2–His5:HB2	2.8	4.6	Pro6:HD1–Pro6:HD2	1.2	1.8
Tyr3:HD[b]–Tyr3:HA	3.0	3.1	Tyr3:HA–Pro6:HD2	3.7	4.0
Tyr3:HD[b]–Arg1:HA	3.8	3.8	His5:HA–Tyr3:HD[b]	4.7	7.5
Tyr3:HD[b]–Tyr3:HB2	2.4	2.4	His5:HN–His5:HB1	2.7	2.9
Tyr3:HE[b]–His5:HA	3.6	4.0	His5:HD2–His5:HB1	2.8	4.6
Tyr3:HE[b]–Tyr3:HB1	3.2	4.2	Tyr3:HD*–Tyr3:HB1	2.4	2.4

[a] Refined using IRMA.
[b] Represent the pseudo-atoms.

Table 2. Inter-proton distances[a] (lower and upper bounds) for VIA in DPC micelles

Proton pair	Distance (Å)		Proton pair	Distance (Å)	
Tyr3 : HN–Val2 : HA	2.1	2.1	His5 : HA–His5 : HB2	3.2	3.4
Tyr3 : HN–Tyr3 : HB2	2.5	2.5	Ile7 : HN–Pro6 : HA	1.9	2.1
Tyr3 : HN–Tyr3 : HB1	2.4	2.4	Val4 : HA–Tyr3 : HB1	2.4	2.6
Tyr3 : HN–Val2 : HB	3.2	4.0	His5 : HB1–Pro6 : HD2	3.3	4.0
Val2 : HN–Arg1 : HA	2.3	2.3	Tyr3 : HA–Val2 : HG[b]	4.0	5.5
Val2 : HN–Val2 : HB	3.0	3.3	Pro6 : HA–Pro6 : HB2	2.8	2.8
His5 : HN–Val4 : HA	1.9	2.0	Pro6 : HA–Pro6 : HB1	2.9	2.9
His5 : HN–His5 : HB1	2.5	2.6	Val2 : HA–Val2 : HB	3.8	3.8
His5 : HN–Val4 : HB	3.2	3.8	Val4 : HA–Val4 : HB	3.2	3.7
Val4 : HN–Tyr3 : HA	2.1	2.1	Pro6 : HB1–Pro6 : HD2	2.2	2.6
Val4 : HN–Tyr3 : HB2	3.0	3.2	Pro6 : HB1–Pro6 : HD1	2.6	2.8
Val4 : HN–Val4 : HB	2.7	3.1	Tyr3 : HN–Val4 : HN	2.9	3.0
Tyr3 : HD[b]–Tyr3 : HA	3.5	3.7	His5 : HN–Val4 : HN	2.9	2.9
Tyr3 : HD[b]–Tyr3 : HB1	2.6	2.7	Tyr3 : HN–Tyr3 : HD[b]	4.0	4.1
His5 : HA–Pro6 : HD2	2.4	2.5	Val4 : HN–Tyr3 : HB1	4.0	5.0
His5 : HA–Pro6 : HD1	2.6	2.6	His + 5 : HN–Pro6 : HD2	3.0	3.7
His5 : HA–His5 : HB1	2.8	2.9	His5 : HN–Pro6 : HD1	3.2	3.9

[a] Refined using IRMA.
[b] Represent the pseudo-atoms.

well known Arrhenius equation:

$$ln\ k = \ln A - \frac{E_a}{T} \quad (2)$$

where k is the exchange rate constant, A is the frequency factor, E_a is the activation energy and T is the absolute temperature.

RESULTS AND DISCUSSION

Resonance assignments

Identification of the spin systems and assignments of individual resonances of VIA in DPC micelles were made with the combined use of DQF-COSY (not shown) and TOCSY (Fig. 1) spectra. Sequence-specific assignment was made using the fingerprint region of the NOESY spectrum (Fig. 2). NOE between CδH of Pro6 and CαH of His5 was used to fix the His5–Pro6 bond in the *trans* position. A similar strategy was employed to assign VIA in water solution (not shown). However, in this case, the ROESY spectrum was used instead of NOESY because the necessary condition $\omega\tau_c \gg 1$ for a good NOESY spectrum is not fulfilled here as compared with the micelle-bound peptide. Chemical shifts for all the resonances of VIA in both water and DPC media are listed in Table 3. It is observed that changing from DPC micelles to water brings about a significant change in the chemical shift ($\Delta\delta$) of NH protons. This change ranges from 0.04 to 0.08 ppm and is largest for His6.

Information about the conformation of the peptide can be deduced from the NMR parameters: chemical shifts (differences from random coil values), ^3J(NH, CαH) coupling constants, hydrogen–deuterium exchange rates and nuclear Overhauser effects. For a small peptide such as that studied here, the molecule is expected to exhibit high conformational flexibility and NMR will reveal only the average of all these conformations.

Table 3. Chemical shifts (ppm) of ^{1}H resonances of VIA at pH 3.8 and 298 K[a]

Amino acid residues		Water	DPC micelles
Arg1	CαH	4.05	4.05
	CβH	1.89	1.84
	CγH	1.50	1.50
	δCH_2, εNH	3.11, 7.07	3.15, 7.10
Val2	NH	8.53	8.53
	CαH	4.18	4.18
	CβH	2.00	2.00
	CγH	0.94	0.92
Tyr3	NH	8.60	8.55 (0.05)
	CαH	4.63	4.62
	CβH	2.98, 3.00	2.98, 2.91
Val4	NH	8.06	8.02 (0.04)
	CαH	4.04	4.05
	CβH	1.94	1.96
	CγH	0.86	0.86
His5	NH	8.46	8.38 (0.08)
	CαH	4.90	4.89
	CβH	3.22	3.21
Pro6	CαH	4.52	4.46 (0.06)
	CβH	2.38, 2.03	2.38, 2.03
	CγH	2.03	2.03
	δCH_2	3.86, 3.55	3.83, 3.58
Ile7	NH	8.02	7.98 (0.04)
	CαH	4.18	4.17
	CβH	1.88	1.88
	CγH	1.46, 1.23	1.46, 1.20
	γCH_3, δCH_3	0.94, 0.94	0.93, 0.93

[a] Numbers in parentheses indicate differences in the chemical shift of the particular protons in water and in DPC micellar medium.

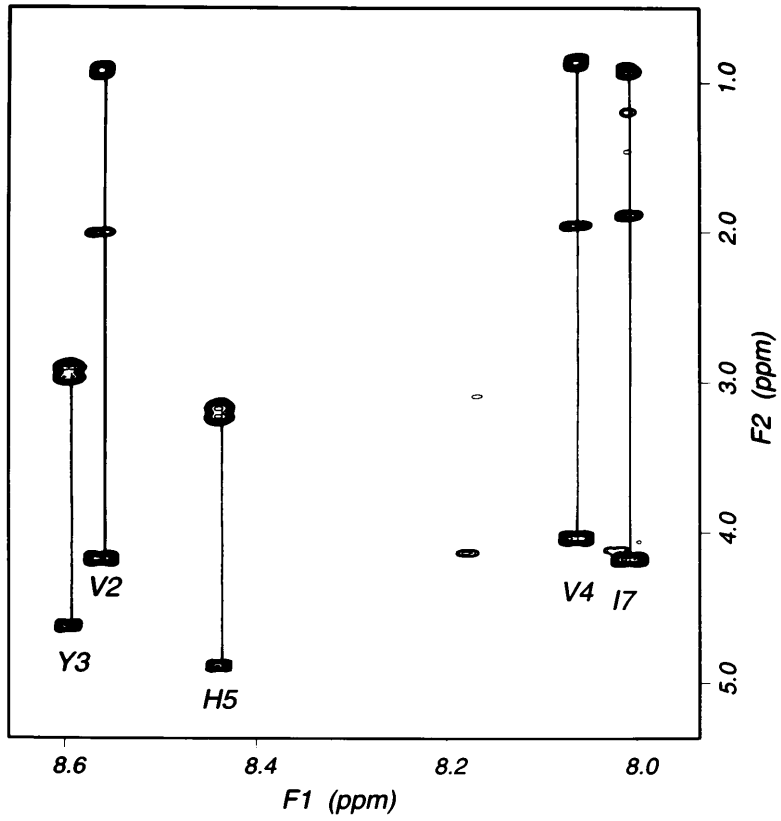

Figure 1. NH region of TOCSY spectrum of VIA in DPC micelles showing correlations. The NH–CαH cross peaks are labeled with single-letter codes for amino acids.

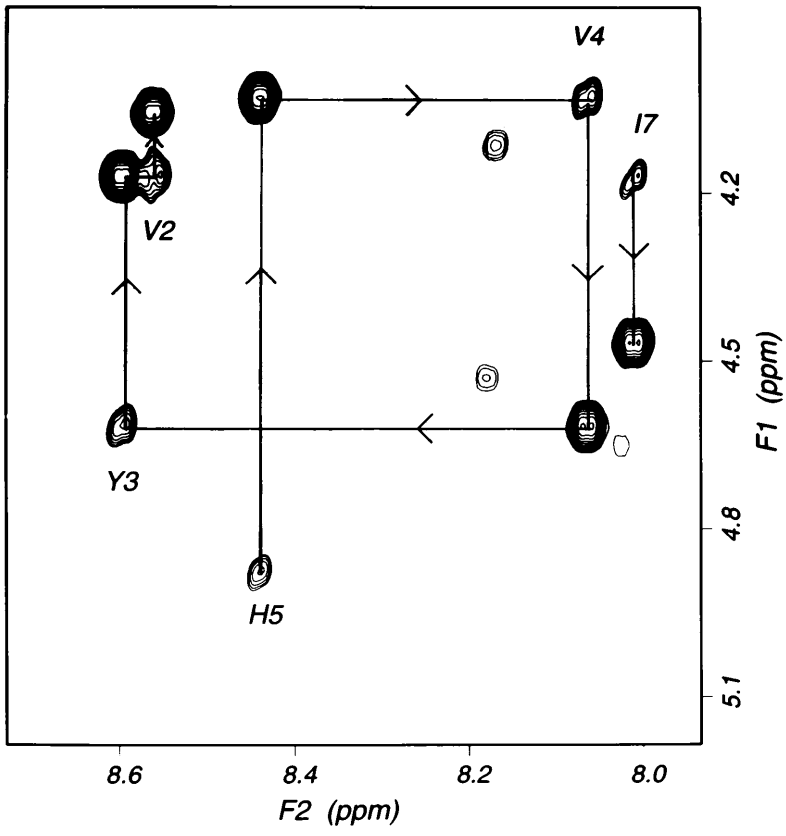

Figure 2. Illustration of the sequential assignment using NOESY spectrum of VIA in DPC micelles. Sequential $d_{\alpha N(i,\, i+1)}$ connectivities are indicated for residues 2–7.

Coupling constants

The ^3J(NH,CαH) coupling constants were measured from the 1D spectrum. These are observed to range from 7 to 8 Hz, in both water and miceller medium. The ^3J(NH,CαH) coupling constants are related to the dihedral angle ϕ by the Karplus relation. However, ϕ is not uniquely determined and must be considered in conjunction with other NMR parameters.

NOE data

The NOESY spectrum of the peptide recorded in water at different mixing times does not show any NOEs. This could be due to intermediate tumbling of the molecule in water. However, a ROESY spectrum where the τ_c dependence of the intensity of the cross peaks is relatively smaller was used for both assignment and structural analysis. Figure 3 shows a survey of the ROEs and NOEs observed for VIA in water and DPC micellar media, respectively. All expected NH_i–CβH_i and some NH_{i+1}–CβH_i NOE cross peaks could be identified in the ROESY/NOESY spectra. The NH–NH region of the ROESY spectrum of the peptide in water and the corresponding region of the NOESY spectrum of the peptide incorporated into DPC micelles are shown in Fig. 4(a) and (b), respectively. Interestingly, two additional strong NH–NH NOEs are seen between NH of Tyr3 and Val4 and between Val4 and His5 in NOESY spectrum of the peptide in DPC micellar medium [Fig. 4(b)], which are not seen in the NOESY/ROESY spectra of the peptide in water. This clearly indicates that there are differences in the structure of the peptide in the two different media.

NH exchange rate

We carried out hydrogen exchange (k_{ex}) studies for the individual amide protons both in micelles and in water over the temperature range 277–292 K. In water, the NH protons exchange too fast and cannot be measured. However, in micelles, the NH protons exchange at a much slower rate and could be monitored with time (Table 4). This observation suggests that some of the amide groups are either buried or involved in hydrogen bond formation.[4] The Arrhenius plots of the exchange rates (k_{ex}) of NH protons with D_2O are shown in Fig. 5. It is unusual for a small peptide to show measurable levels of amide protection from deuterium exchange as observed here. This suggests the presence of a stable

Table 4. Deuterium exchange rate of NH protons of VIA in DPC micelles

Residue	Exchange rate (min^{-1}) $\times 10^{-2}$
Val2	54.60 ± 3.50
Tyr3	26.60 ± 0.20
Val4	16.10 ± 0.10
His5	10.10 ± 0.40
Ile7	7.00 ± 0.27

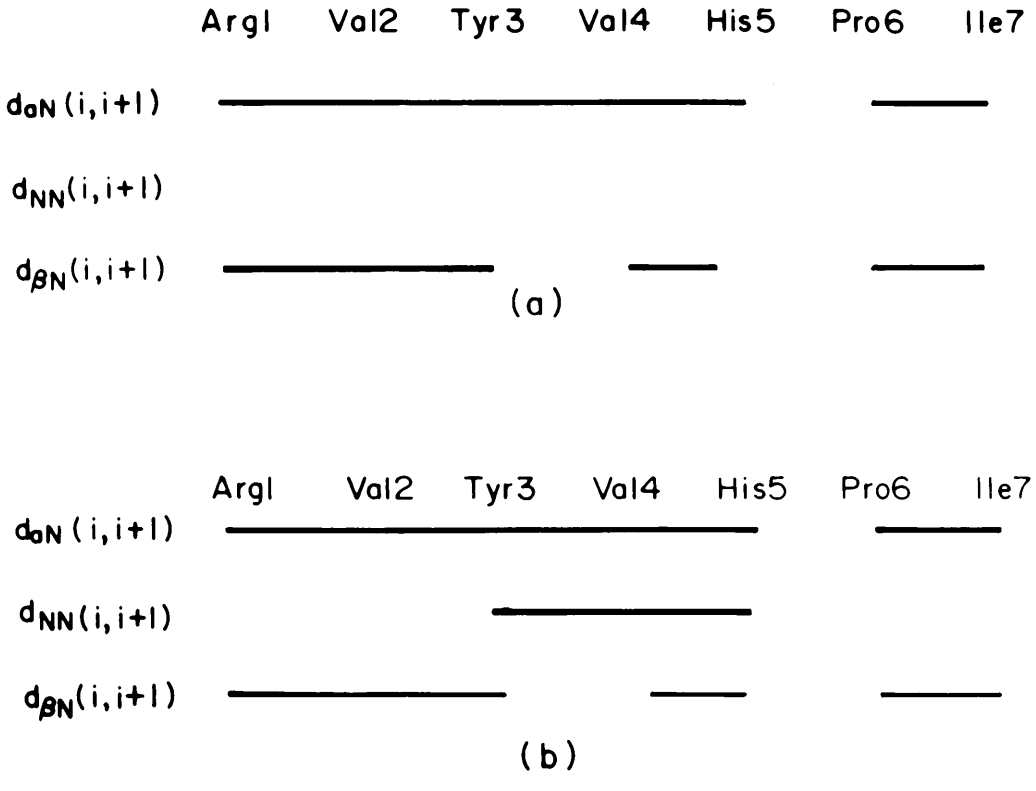

Figure 3. Summary of the (a) observed ROEs for VIA in water and (b) TRNOEs detected for the micelle-bound peptide.

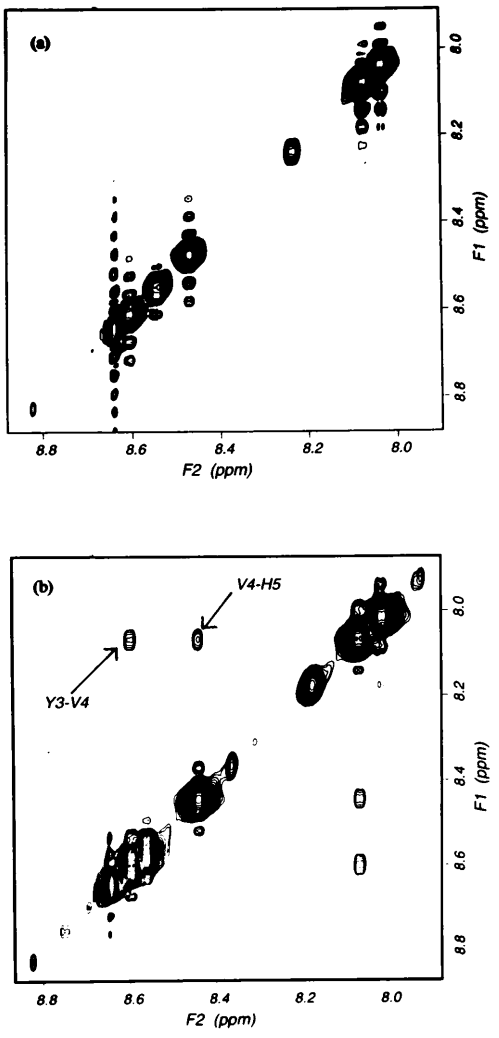

Figure 4. NH–NH region of the VIA: (a) ROESY spectrum in water and (b) NOESY spectrum in DPC micelles.

peptide structure in DPC micelles. The exchange rate (k_{ex}) data for amide protons of the peptide in micelles can be categorized into two groups, the first group comprising Val4, His5 and Ile7 with corresponding rate constants of 16.1, 10.1 and 7.0 and the other group of Tyr3 and Val2 with corresponding rate constants of 26.6 and 54.6 at 287 K. The latter are 2–3-fold higher than the former. This indicates that although all the NH protons experience solvent shielding and exchange slowly in the micellar environment, the lower k_{ex} values for Val4, His5 and Ile7 NHs are possibly due to their involvement in hydrogen bonding.

Conformation

For a given set of NOEs, the accuracy of structures generated can be improved by deriving more precise distance constraints from experimental data. The observed distances from NOEs and ROEs in the two cases were refined using IRMA methodology and used as distance constraints in the molecular dynamics simulations as discussed in the experimental section. The r.m.s.d. values obtained after each refinement step with the final step of IRMA and *R*-factor at different cycles of IRMA are listed in Table 5. It is apparent that the *R*-factor decreases slowly and then levels off. Also, as the structures start to improve in terms of violations of the NOE constraints, the r.m.s. differences gradually become smaller. Using refined distances (Tables 1 and 2), restrained MD calculations were carried out. Energies of the structures taken from the trajectory of a 100 ps molecular dynamics simulation in water and DPC micelles are shown in Fig. 6(a) and (b), respectively. All

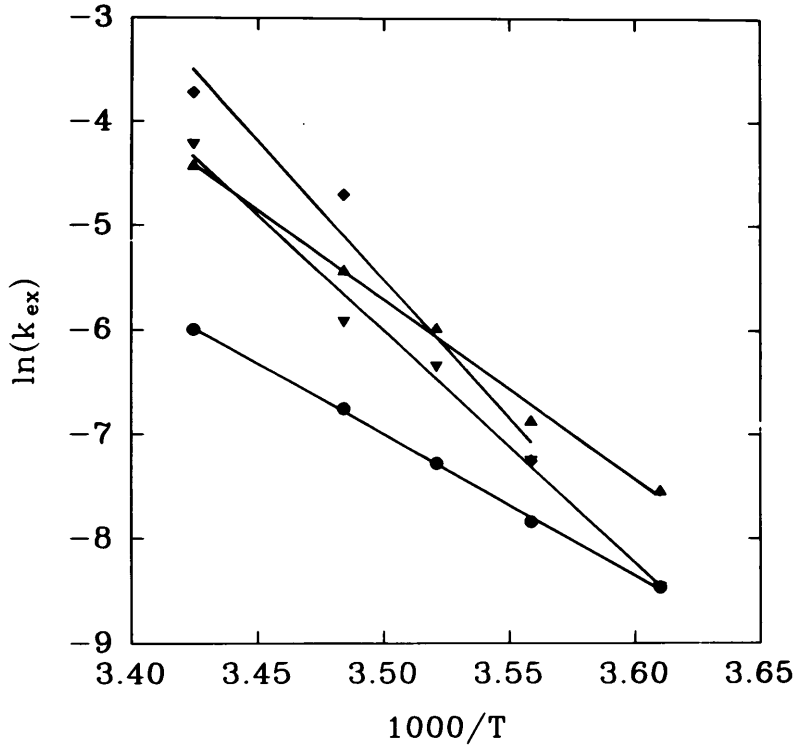

Figure 5. Arrhenius plot of the exchange rates (k_{ex}) of NH protons in VIA in DPC micelles with D_2O.

Table 5. *R*-factor and root mean square differences (r.m.s.ds[a]) of atomic coordinates (Å) for structures after various cycles of IRMA procedure

	Water			DPC		
		R.m.s.d.			R.m.s.d.	
Cycle	*R*-factor	Heavy atom	Backbone	*R*-factor	Heavy atom	Backbone
0	—	5.057	4.056	—	3.065	2.047
1	0.590	0.958	0.476	0.336	0.395	0.391
2	0.536	1.347	0.437	0.278	0.644	0.371
3	0.574	0.021	0.017	0.279	0.354	0.356
4	0.462	0.021	0.017	0.287	0.080	0.030

[a] R.m.s.d. was calculated from the final structure.

the 100 structures generated by restrained MD simulation were analyzed. All structures satisfy the experimental constraints fairly well. Only a few constraints were violated by more than 0.2 Å and none by more than 0.3 Å. The conformational parameters for the averaged structure together with the r.m.s. deviation seen for the dihedral angles for the whole trajectory for VIA in DPC and water media are given in Tables 6 and 7, respectively. Good homogeneity in the structures generated by constrained MD simulation is observed. In the case of DPC medium, the structures display a non-specific turn around Val4. The turn is stabilized by hydrogen bonding between Tyr3CO and His5NH. This observation is well supported by the change in chemical shifts and k_{ex} values measured for the amide protons, where Val4 and His5 exhibit a significantly low deuterium exchange rate. On the other hand, the analysis of the constrained MD simulation of VIA in water showed more of an extended structure. The global minimum energy structures of VIA generated by MD simulation in water and DPC matrix are shown in Fig. 7(a) and (b), respectively. The backbone torsion angles (ϕ, φ) and side-chain torsion angles (χ_i) for these structures are listed in Tables 8 and 9.

Literature reports on the conformation of angiotensin III and II and its analogues based on CD and ^{1}H NMR data[20] indicate that the segment Val–Tyr–Ile–His adopts a unique structure which is recognized by the receptor. This conclusion is supported by the observation that both the Tyr and His side-chains are essential for the biological activity of these peptides.[2,3,21,22] In VIA, the replacement of Ile4 by Val4 and Phe7 by

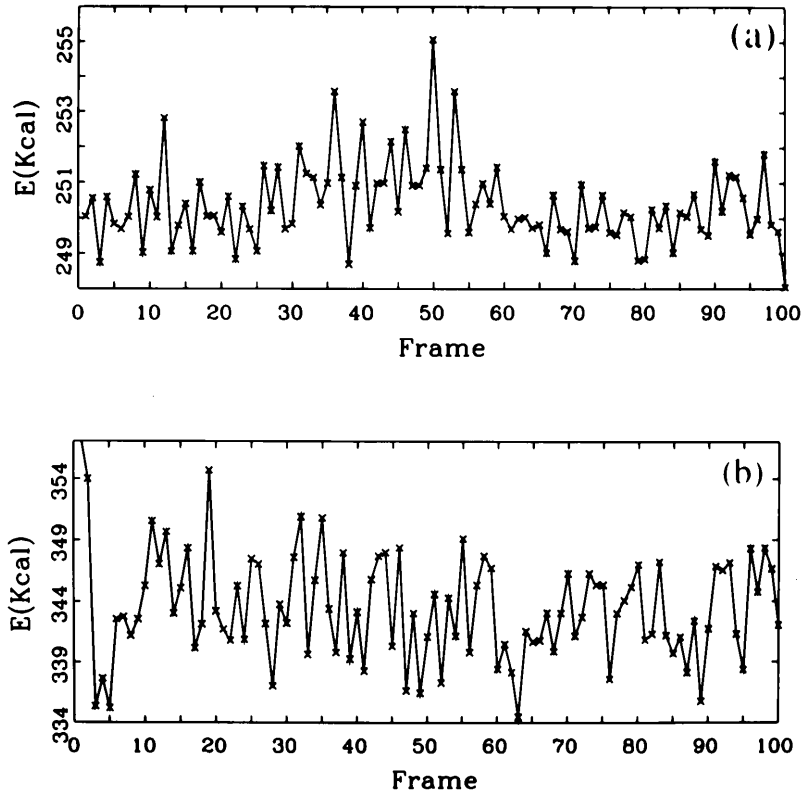

Figure 6. Energy of the VIA structures taken from the trajectory of a 100 ps molecular dynamics simulation in (a) water and (b) DPC micelles.

Table 6. Averaged torsion angles with r.m.s.d. for VIA in DPC micelles as determined by restrained MD simulations

Amino acid	Torsion angle (°)						
	ϕ	φ	χ_1	χ_2	χ_3	χ_4	χ_5
Arg1	—	114 ± 10	-166 ± 11	70 ± 15	-100 ± 19	-136 ± 40	178 ± 14
Val2	-138 ± 8	125 ± 3	-38 ± 5	-55 ± 12	52 ± 6		
Tyr3	-135 ± 17	145 ± 4	-84 ± 2	120 ± 35	174 ± 10		
Val4	86 ± 1	-87 ± 4	163 ± 1	165 ± 20	-178 ± 3		
His5	-171 ± 3	86 ± 7	171 ± 2	-86 ± 24			
Pro6	-82 ± 4	140 ± 11	-37 ± 2				
Ile7	149 ± 13	—	-75 ± 50	65 ± 3	90 ± 50		

Table 7. Averaged torsion angles with r.m.s.d. for VIA in water as determined by restrained MD simulation

Amino acid	Torsion angle (°)						
	ϕ	φ	χ_1	χ_2	χ_3	χ_4	χ_5
Arg1	—	177 ± 1	146 ± 39	-60 ± 20	129 ± 61	-139 ± 42	179 ± 1
Val2	-98 ± 1	81 ± 1	-165 ± 19	66 ± 5	70 ± 2		
Tyr3	-149 ± 1	89 ± 1	-178 ± 9	-103 ± 7	-3 ± 2		
Val4	-103 ± 1	82 ± 1	-168 ± 1	54 ± 10	-169 ± 2		
His5	-31 ± 7	119 ± 1	-174 ± 1	-133 ± 2			
Pro6	-121 ± 3	159 ± 1	26 ± 1				
Ile7	-112 ± 5	—	-168 ± 3	-57 ± 3	68 ± 1		

Table 8. Torsion angles of lowest energy structure of VIA in DPC as determined by restrained MD simulations

Amino acid	Torsion angle (°)						
	ϕ	φ	χ_1	χ_2	χ_3	χ_4	χ_5
Arg1	—	104	−177	60	−82	172	−177
Val2	−151	124	−48	−55	54		
Tyr3	−127	150	−81	124	179		
Val4	84	−94	161	175	−179		
His5	−166	−87	170	−92			
Pro6	−81	120	−37				
Ile7	150	—	−55	64	53		

Table 9. Torsion angles of lowest energy structure of VIA in water as determined by restrained MD

Amino acid	Torsion angle (°)						
	ϕ	φ	χ_1	χ_2	χ_3	χ_4	χ_5
Arg1		−178	169	−54	174	−146	179
Val2	−102	81	−167	−66	70		
Tyr3	−149	90	−180	−105	−3		
Val4	−103	82	−168	54	−170		
His5	−31	119	−174	−134			
Pro6	−121	159	51				
Ile7	−111	—	−170	−54	64	55	

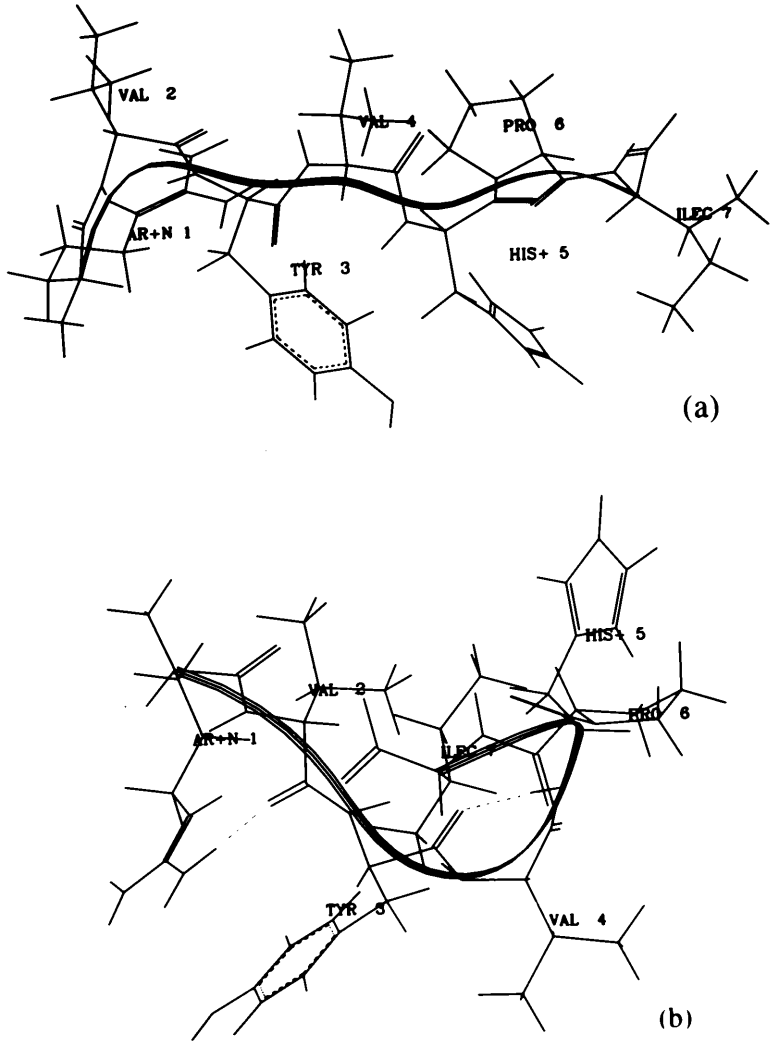

Figure 7. Conformation of VIA simulated using refined distance constraints in (a) water and (b) DPC micelles. The broken lines represent H-bonds.

Ile7 brings about a change in the conformation of the peptide in water without conferring any unique structure to the tetrad. However, in micellar media the *C*-terminal tetrad has a distinctive structure with a bend involving Tyr3, Val4 and Pro6 residues. Micellar media being closer to the actual situations, one can infer that the replacements do not adversely effect the biological efficacy of the peptide.

The characterization of the structural elements responsible for the specific receptor interaction and for the induction of the biological response is of great pharmacological interest. The interaction of hormones with the membrane-embedded receptor molecules could involve intermediate steps, such as accumulation, structuring and orientation of the peptide in the membrane prior to its binding to the receptor. The membrane-induced conformation of VIA in our study may contribute to further elucidation of the specific peptide receptor interaction, as it may guide the design of new analogues, mimicking the membrane-bound conformation. The results of such investigations will be very interesting as they could help in evaluating the structural role of the membrane interactions.

CONCLUSIONS

VIA in water shows no NOEs and weak intra-residue ROEs. On the other hand, in DPC micelles, a large number of NOEs including inter-residue NOEs could be observed. This and other NMR parameters, notably the deuterium exchange rates, indicate that the micellar environment imparts a unique conformation to the peptide. Structures generated using restrained MD simulation show a conformation with a non-specific bend for the peptide in micelles compared with a nearly extended structure in water.

Acknowledgements

The facilities provided by the National Facility for High Field NMR located at TIFR, Mumbai, are gratefully acknowledged.

REFERENCES

1. M. Shimamura, K. Kawamuki and T. Hazato, *J. Neurochem.* **49**, 536 (1987).
2. M. J. Peach, *Physiol. Rev.* **57**, 313 (1977).

3. M. C. Khosla, R. R. Smeby and F. M. Bumpus, in *Handbook of Experimental Pharmacology*, Vol. 37, p. 126. Springer, Berlin (1973).
4. K. Wuthrich, *NMR of Proteins and Nucleic Acids*, Wiley–Interscience, New York (1986).
5. U. Piantini, O. W. Sorensen and R. R. Ernst, *J. Am. Chem. Soc.* **104**, 6800 (1982).
6. L. Braunschweiler and R. R. Ernst, *J. Magn. Reson.* **53**, 521 (1983).
7. A. Bax and D. G. Davis, *J. Magn. Reson.* **65**, 355 (1985).
8. J. Jeener, B. H. Meier, P. Bachmann and R. R. Ernst, *J. Chem. Phys.* **71**, 4546 (1979).
9. A. A. Bothner-By, R. L. Stephens, J. Lee, C. D. Waren and R. W. Jeanloz, *J. Am. Chem. Soc.* **106**, 811 (1984).
10. A. Bax and D. G. Davis, *J. Magn. Reson.* **65**, 355 (1985).
11, D. J. States, R. A. Haberkorn and D. J. Ruben, *J. Magn. Reson.* **48**, 286 (1982).
12. J. Maple, U. Dinur and A. T. Hagler, *Proc. Natl. Acad Sci. USA* **65**, 5350 (1988).
13. G. M. Clore and A. M. Gronenborn, *J. Magn. Reson.* **53**, 423 (1983).
14. A. P. Campbell and B. D. Sykes, *J. Magn. Reson.* **93**, 77 (1991).
15. G. M. Lippens, C. Cerf and K. Halenga, *J. Magn. Reson.* **99**, 268 (1992).
16. R. E. London, M. E. Perlman and D. G. Davis, *J. Magn. Reson.* **97**, 79 (1992).
17. R. Boelens, T. M. G. Koning, G. A. van der Marel, J. H van Boom and R. Kaptein, *J. Magn. Reson.* **82**, 290 (1989).
18. L. Verlet, *Phys. Rev.* **159**, 98 (1967).
19. S. W. Englander and N. R. Kallenbach, *Q. Rev. Biophys.* **16**, 521 (1984).
20. R. E. Lenkinski, R. L. Staphens and N. R. Krishna, *Biochim. Biophys. Acta* **667**, 157 (1981).
21. P. Piriou, L. Lintner, S. Fermandjian, P. Fromageot, M. C. Khosla, R. R. Smeby and F. M. Bumpus, *Proc. Natl. Acad. Sci. USA* **77**, 82 (1980).
22. D. Regoli, W. K. Park and F. Rioux, *Pharmacol. Rev.* **26**, 69 (1974).

